JOURNAL OF COMPUTATIONAL PHYSICS **128,** 121–133 (1996)
ARTICLE NO. 0199

Direction-Adaptive Nonreflecting Boundary Conditions

PAOLO LUCHINI* AND RENATO TOGNACCINI†

**Dipartimento di Ingegneria Aerospaziale, Politecnico di Milano, Milan, Italy; †Dipartimento di Progettazione Aeronautica, Università degli Studi di Napoli "Federico II," Naples, Italy*

Received June 7, 1995; revised May 2, 1996

Presented in this work is a nonlinear adaptive nonreflecting boundary condition (NRBC) that, when compared with classical local NRBCs, further reduces the wave reflection error at far fields in the numerical simulation of wave dominated problems. A nonlinear procedure can considerably improve the accuracy of NRBCs even if the problem itself is linear as in the case of the 2D wave equation. In fact the first- and second-order NRBCs of Engquist and Majda can be modified by adding proper weights to the coefficients of the difference equations. The weights are adaptively determined in such a way that the angle of complete absorption is locally coincident with the outgoing wave direction. The theoretical reflection coefficients and the numerical experiments show that a considerable reduction of the numerical error due to wave reflections is achieved by applying the present adaptive algorithm.

1. INTRODUCTION

While reading, some time ago, an interesting review paper on nonreflecting boundary conditions (NRBCs) [1], our attention was struck by the fact that only linear methods appear to have been investigated. Despite the fact that it may at first look awkward to propose a nonlinear discrete approximation to a linear differential problem, there are some practical advantages in adopting one. The purpose of this article is to illustrate a nonlinear type of NRBC.

As may also be read in [1], there is some vagueness in the concept of NRBC, and even a number of different names to denote it. Despite the fact that the basic philosophy of NRBCs is derived from Sommerfeld's radiation condition for the wave equation, they serve a quite different purpose: Sommerfeld's condition is imposed at infinity in order to make a radiation problem well-posed and uniquely determined from the mathematical viewpoint, whereas numerical NRBCs are imposed at a finite artificial boundary in order to let the numerical solution of the thus truncated problem approximate, as well as possible, a continuous solution that is defined in an infinite domain. It follows that NRBCs necessarily embody at least some information about the neglected exterior part of the calculation domain and are more or less precisely defined, depending on how thoroughly one is willing, or able, to specify the properties of the exterior.

If the exterior domain has a simple shape, say the exterior of a circle or sphere, and the differential equations of the problem are simple as well, say the constant-coefficient D'Alembert wave equation, it may turn out that it is possible to solve the exterior problem analytically (Sommerfeld's radiation condition is used at this stage) and to express the solution as an integral condition over the boundary. Such a condition is nonlocal in space, as well as in time, involving values of the variables along all the boundary at present and past instants. It is called in [1] an exact nonlocal NRBC. Whereas such exact nonlocal NRBCs are in a mathematical sense the best possible solution of the problem, they are computationally cumbersome and, even more important, are only available for simple problems with constant properties. A spatial variation of the coefficient of the wave equation is already sufficient to destroy the exactness of these NRBCs as is a more complicated shape of the boundary (recent progress in this field can be found in [2]).

On the other hand, local NRBCs try to embody the intuitive, but for most problems not mathematically rigorous, idea that waves travelling away from their sources must traverse artificial numerical boundaries in the outward direction causing no reflected inward wave (whence the name of nonreflecting boundary conditions). This concept may be stated precisely and locally in the limit of plane waves of infinitesimal wavelength and all local NRBCs are mathematically justified with reference to this limit only. In fact, in order to separate the effect of a portion of the artificial boundary from the rest and thus formulate a local condition that can work as well for inhomogeneous problems, it is necessary to invoke the assumption of locally plane waves of infinitesimal wavelength because only under this assumption can the general nonlocal, Green function integral be reduced to a small neighbourhood of the boundary point considered. This does not mean, however, that local NRBCs should be rejected as intrinsically inaccurate: all waves become more and more locally plane as

0021-9991/96 $18.00

they travel farther and farther away from their sources; and the ratio of their wavelength to the typical dimension of the boundary becomes smaller and smaller as the boundary itself is allowed to grow in size. By choosing the artificial boundary for a local NRBC appropriately, its approximation may be matched to the other approximations that are intrinsic in a numerical calculation (discretization, etc.), so that its use in this context is acceptable. In addition to being simpler, local NRBCs are much more flexible than nonlocal ones because, just as a consequence of their locality, they can easily be adapted to spatially and/or temporally nonhomogeneous problems and to different shapes of the boundary.

Even once the problem of constructing an NRBC has been restricted to considering locally plane waves of small wavelength, an important degree of freedom remains in the direction of such waves. A great number of different NRBCs were developed following and modifying Engquist and Majda's idea [3] of interpolating the desired branch of the dispersion equation by a rational function. Indeed, such local NRBCs turn out to be exactly nonreflecting for a number of discrete directions and just approximately so for all others. It was proved by Higdon [4, 5] that all the NRBCs derived from Engquist and Majda's approach may be reduced to the single formula

$$\prod_{j=1}^{m} \left[\cos(\theta_j) \frac{\partial}{\partial t} - c \frac{\partial}{\partial x} \right]_{x=0} u = 0 \tag{1.1}$$

(in the case of the scalar wave equation, or corresponding formulae for higher order wave equations), in the sense that they either can be directly represented by this formula or admit a better variant that can (see also [1]). In Eq. (1.1) x is the coordinate normal to the boundary (defined by $x = 0$) and c is the propagation speed; the parameters θ_j, which may be chosen at will, are the angles of zero reflection.

The method we propose in this paper is based on the observation that it is "unlikely" that waves hitting any given small region of the boundary at any given time may come from more than one direction with significant amplitude. In fact, this imprecise concept of unlikelihood is just what is meant by saying that waves tend to become locally plane and, consistent with the other assumptions that are made in adopting a local NRBC, grow more and more precise with increasing size of the artificial boundary. Just as Sommerfeld's condition, this property becomes exactly true in the limit of size tending to infinity, when the standard asymptotic analysis of the wave equation shows that only a single plane wave is seen in each direction (what is called the Fraunhofer limit in optical terminology).

As was recalled above, a linear local NRBC that is exactly nonreflecting for a number of given directions is easily constructed, for instance from a numerical discretization of Eq. (1.1). But, if we allow the condition to be nonlinear, we can "measure" in some way the prevailing direction of propagation of waves that hit the boundary at any particular location of space and time and automatically make this direction one of those of zero reflection. The resulting NRBC will by construction be very effective wherever the waves are characterised by a well-defined direction of propagation. In the spots of space and time where this does not happen its performance will fall back, but never below that of a generic linear NRBC with angles of zero reflection chosen without a particular criterion. In our opinion such occasions are exceptional and of limited spatial and temporal extent for, on a sufficiently far boundary, waves of different direction tend to separate from each other.

The proposed algorithm can be specialised for any given space-time integration scheme in a straightforward way. In the next section a first- and a second-order nonlinear adaptive NRBC are presented; particular difference expressions have been derived for a scheme with a time-staggered grid that we have chosen for the tests. In Section 3 some applications of the proposed BCs are shown and discussed using the test cases proposed by Higdon in [4] to illustrate the effects of the outgoing wave direction on the accuracy of NRBCs.

2. NONLINEAR ADAPTIVE NRBCS

In order to test the concept of a nonlinear adaptive NRBC, let us consider a very simple time-staggered finite-difference central discretization of the two-dimensional wave equation

$$u_{tt} = u_{xx} + u_{yy}, \tag{2.1}$$

to be solved in the domain $x > 0$ by the explicit formula

$$\begin{aligned} u_{i,j}^{(n+1)} = -u_{i,j}^{(n-1)} + \tfrac{1}{2} [& u_{i+1/2,j+1/2}^{(n)} \\ & + u_{i-1/2,j+1/2}^{(n)} + u_{i-1/2,j-1/2}^{(n)} + u_{i+1/2,j-1/2}^{(n)}], \end{aligned} \tag{2.2}$$

where $u_{i,j}^{(n)}$ represents the unknown calculated at position (ih, jh) and time $n\Delta t$, and the time and space steps are related to each other as $\Delta t = h/2$. More complicated discretizations might be chosen in order to allow the use of unconstrained time and space steps, or of a space-varying wave speed, but they would hide rather than clarify the role of the nonreflecting boundary condition.

Equation (2.2) is a nondissipative, second-order accurate approximation to the wave equation (2.1), as is easily checked by Fourier-transforming with respect to both coordinates and time and then comparing the resulting disper-

sion equation

$$\cos(\omega\Delta t) = \cos(\alpha h/2)\cos(\beta h/2) \tag{2.3}$$

with that of the continuous wave equation

$$\omega^2 = \alpha^2 + \beta^2, \tag{2.4}$$

where α and β are the components of the wave vector $\mathbf{k}$ and ω is the angular frequency. The phase-speed error vanishes for waves propagating along either coordinate axis and remains less than 1% in all directions for wavenumbers smaller than $1/h$.

This algorithm is characterized by the use of a constrained time step. However, it has the interesting property that the numerical accuracy is improved by use of a more compact stencil of the discrete Laplace operator while retaining the same number of grid points. In fact, the staggered grid provides a reduction of the effective spacing by a factor $\sqrt{2}$ as can be verified by comparing the dispersion relation (2.3) with that of other, nonstaggered, schemes.

The basic nonreflecting analytical boundary conditions that can be associated with Eq. (2.2) at the boundary $x = 0$ are given by

$$\left[\frac{\partial}{\partial t} - \frac{\partial}{\partial x}\right]^m_{x=0} u = 0. \tag{2.5}$$

With $m = 1$ and $m = 2$, the first- and second-order Engquist and Majda's boundary conditions are obtained respectively [4].

2.1. *First-Order Method*

The natural discretization of Eq. (2.5) for the case $m = 1$ on a time-staggered mesh is expressed by

$$u^{(n+1)}_{0,j} = \tfrac{1}{2}[u^{(n)}_{1/2,j-1/2} + u^{(n)}_{1/2,j+1/2}]. \tag{2.6}$$

It can easily be verified by substitution that this condition does not reflect plane waves travelling parallel to the x-axis in the decreasing-x direction. (It is exactly satisfied by such waves and, therefore, no backward waves need to appear at the boundary in order to satisfy the boundary condition.) When waves hit the boundary obliquely, however, Eq. (2.6) generates considerable reflection.

The reflection coefficient of this and other boundary conditions can easily be computed by imposing that a linear combination of an incoming (reflected) and outgoing wave of the form

$$\hat{u}^{(n)}_{i,j} = (e^{I\omega\Delta t})^n\,(e^{-I\alpha h})^i\,(e^{-I\beta h})^j = z^n k^i l^j, \quad I = \sqrt{-1}, \tag{2.7}$$

perfectly satisfy Eq. (2.6) (see, for instance, the already cited work of Higdon). Its expression is

$$R = -\frac{[z - \tfrac{1}{2}k_2^{1/2}(l^{-1/2} + l^{1/2})]}{[z - \tfrac{1}{2}k_1^{1/2}(l^{-1/2} + l^{1/2})]}, \tag{2.8}$$

where $k_1 = \exp(-I\alpha_1 h)$ and $k_2 = \exp(-I\alpha_2 h)$ are respectively associated to the incoming and outgoing waves. In Eq. (2.8) the phase speed ω is related to the wave vector components (α_k, β) by the dispersion relation (2.3). The reflection coefficient for large wavelengths, i.e., for waves well resolved by the grid, can be approximated by applying Taylor expansions to z, k_k, and l, obtaining a direct connection with the outgoing wave direction θ (measured with respect to the outward normal of the boundary):

$$R \approx -\frac{(\omega + \alpha_2)}{(\omega + \alpha_1)} = -\frac{(1 - \cos\theta)}{(1 + \cos\theta)}, \tag{2.9}$$

since for large wavelengths the dispersion relation of the scheme tends towards the continuous one and $\alpha_2/\omega \approx -\cos\theta$, $\alpha_1/\omega \approx \cos\theta$.

To reduce the wave reflection, the nonlinear adaptive strategy may be applied. As a first step, Eq. (2.6) is transformed into a condition that is nonreflecting for plane waves arriving from a general prescribed single direction. The simplest way to achieve this aim is to attach suitable weights $w^{(-)}$ and $w^{(+)}$ to the values on the r.h.s. of Eq. (2.6), thus rewriting this equation as

$$u^{(n+1)}_{0,j} = \tfrac{1}{2}[w^{(-)}u^{(n)}_{1/2,j-1/2} + w^{(+)}u^{(n)}_{1/2,j+1/2}]. \tag{2.10}$$

A similar procedure can be applied to any other chosen discretization of the wave equation by replacing $\partial/\partial x$ in Eq. (2.5) by a weighted combination of first derivatives computed in two different spatial direction. Let now $\hat{\mathbf{d}} = (-\cos\theta, \sin\theta)$ be a general unit vector. We wish to determine $w^{(-)}$ and $w^{(+)}$ in such a way that Eq. (2.10) may constitute an exact NRBC for waves travelling in the direction $\hat{\mathbf{d}}$. A plane, not necessarily sinusoidal, wave travelling in this direction is represented by a function of the form $u = f(t + x\cos\theta - y\sin\theta)$. In order that no reflection should occur, Eq. (2.10) itself must be satisfied (to leading order in its Taylor-series expansion, at least, consistently with the principle of difference approximation) by this single travelling wave.

Expanding the function f in a Taylor series as

$$f = f_0 + f_0' \cdot [(t - t_0) + (x - x_0)\cos\theta - (y - y_0)\sin\theta] + \tfrac{1}{2}f_0'' \cdot [(t - t_0) + (x - x_0)\cos\theta - (y - y_0)\sin\theta]^2 \tag{2.11}$$

and inserting the constant and the linear term into Eq. (2.10) gives

$$[1 - \tfrac{1}{2}(w^{(-)} + w^{(+)})]f_0 + [\Delta t - \tfrac{1}{4}(w^{(-)} + w^{(+)})h \cos\theta - \tfrac{1}{4}(w^{(-)} - w^{(+)})h \sin\theta]f_0' = 0. \tag{2.12}$$

Then, equating the coefficients of f_0 and f_0' separately to zero and remembering that $\Delta t = h/2$, we obtain the two equations,

$$w^{(-)} + w^{(+)} = 2, \tag{2.13.a}$$

$$(\sin\theta + \cos\theta)w^{(-)} + (\cos\theta - \sin\theta)w^{(+)} = 2, \tag{2.13.b}$$

from which $w^{(-)}$ and $w^{(+)}$ may be calculated as functions of θ, finally yielding

$$w^{(-)} = 1 + \frac{1 - \cos\theta}{\sin\theta}, \tag{2.14.a}$$

$$w^{(+)} = 1 - \frac{1 - \cos\theta}{\sin\theta}. \tag{2.14.b}$$

Incidentally, the boundary condition (2.10) with the weights specified by (2.14), in addition to being nonreflecting for waves coming along the direction $\hat{\mathbf{d}}$, also turns up nonreflecting for waves parallel to the x-axis. Indeed, it may be verified that Eq. (2.13.b) is satisfied for $\theta = 0$, for any choice of $w^{(-)}$ and $w^{(+)}$ consistent with Eq. (2.13.a).

Although we have obtained Eq. (2.14) by working on the discretized equations directly, one may also arrive at the same result by considering the differential form of Eq. (2.10), that is,

$$[2u_t - w^{(-)}(u_x - u_y) - w^{(+)}(u_x + u_y)]_{x=0} = 0. \tag{2.15}$$

It may quickly be checked that this equation is exactly verified by plane waves travelling in the direction $\hat{\boldsymbol{d}}$ as well as by plane waves travelling along the x-axis. It is also possible to show (as suggested to us by one of the reviewers) that Eq. (2.15) is equivalent to Eq. (1.1) specialised for $m = 1$, $\theta_j = \theta/2$ and if the coordinate system is rotated by an angle $\theta/2$. It may be observed that Eq. (2.15), contrary to Higdon's general formula (1.1), contains derivatives parallel to the boundary in combination with derivatives normal to the boundary. We believe that the inclusion of parallel derivatives is beneficial whenever oblique waves are involved.

Once we have obtained a condition that works for locally plane waves of any prescribed direction, the second step is to make this direction a function of the evolving solution itself by adapting it to the local direction of the wave impinging on the boundary. For this purpose, we use the property that, if u has the structure of a locally plane wave, then the gradient of u is directed parallel to the wave vector. We therefore choose the local direction of the discretized gradient as vector $\hat{\mathbf{d}}$ and our NRBC is completely defined.

An efficient expression of Eq. (2.14) in terms of the gradient components avoiding conditional statements and that has been used in our calculations is given by

$$\begin{aligned}
\Delta_1 &= u_{1/2,j+1/2} - u_{3/2,j-1/2}, \\
\Delta_2 &= u_{1/2,j-1/2} - u_{3/2,j+1/2}, \\
\Delta_0 &= \mathrm{sign}(1, \Delta_1 + \Delta_2)\sqrt{\tfrac{1}{2}(\Delta_1^2 + \Delta_2^2)}, \\
w^{(-)} &= \frac{2|\Delta_0 - \Delta_2|}{|\Delta_0 - \Delta_2| + |\Delta_1 - \Delta_0|}, \\
w^{(+)} &= \frac{2|\Delta_1 - \Delta_0|}{|\Delta_0 - \Delta_2| + |\Delta_1 - \Delta_0|}.
\end{aligned} \tag{2.16}$$

During the execution of the numerical experiments we tried different gradient computations without significant differences in the results. An exception is Test 2 (see Section 3) performed by the second-order NRBC to be discussed below. In this case, characterised by very high frequency modes that are not realistic in practical applications, the correct computation of the wave direction was obtained by smoothing the local gradient with the surrounding values.

Finally the reflection coefficient for boundary condition (2.10) with constant weights $w^{(-)}$ and $w^{(+)}$ is given by

$$R = -\frac{[z - \tfrac{1}{2}k_2^{1/2}(w^{(-)}l^{-1/2} + w^{(+)}l^{1/2})]}{[z - \tfrac{1}{2}k_1^{1/2}(w^{(-)}l^{-1/2} + w^{(+)}l^{1/2})]}. \tag{2.17}$$

For large wavelengths its expression reduces to

$$\begin{aligned}
R &\approx -\frac{[\omega + \alpha_2 - \tfrac{1}{2}\beta(w^{(-)} - w^{(+)})]}{[\omega + \alpha_1 - \tfrac{1}{2}\beta(w^{(-)} - w^{(+)})]} \\
&= -\frac{[1 - \cos\theta - \tfrac{1}{2}\sin\theta(w^{(-)} - w^{(+)})]}{[1 + \cos\theta - \tfrac{1}{2}\sin\theta[(w^{(-)} - w^{(+)})]}.
\end{aligned} \tag{2.18}$$

This relation also provides the reflection coefficient of the analytical BC (2.15). In Fig. 1 $|R|$, as expressed by Eq. (2.18), is plotted versus θ. The behaviour of $|R|$ for case ($w^{(-)} = 1$, $w^{(+)} = 1$) and for the case ($w^{(-)} = 1.41$, $w^{(+)} = 0.59$) are compared. The second condition corresponds to weight values adapted to 45° incident waves. As expected, in this case $|R| = 0$ also for $\theta = 45°$. By choosing for each θ the weight values given by (2.14) the resulting diagram is, as is obvious, $|R| = \text{const} = 0$. The same results are presented in Fig. 2 by using Eq. (2.17) with wave number $|\mathbf{k}| = \pi/(2h)$; in this case $|R|$ no more equals zero for $\theta =$

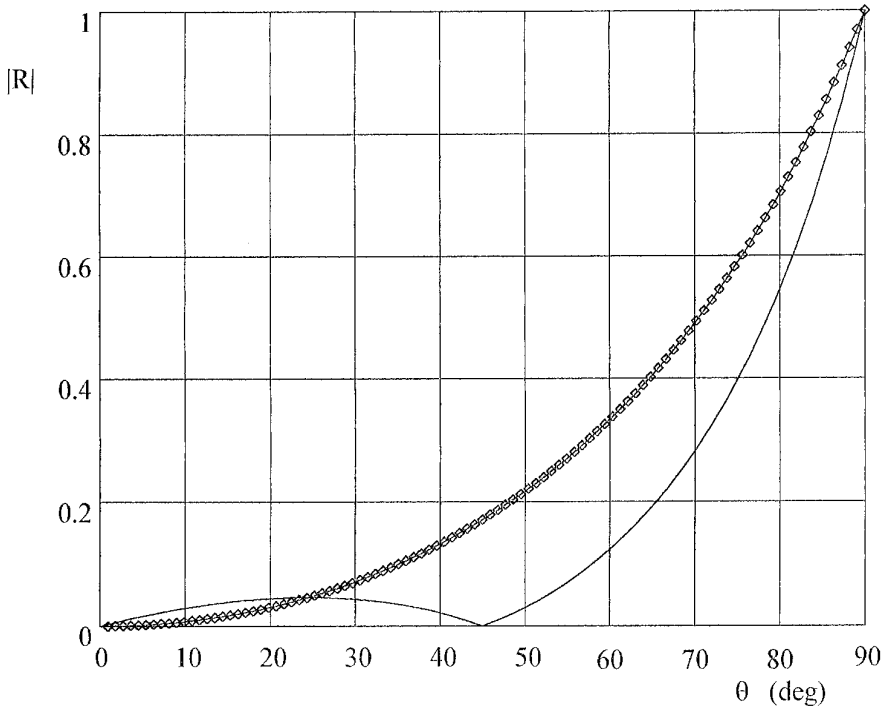

FIG. 1. First-order NRBCs, $|R|$ versus θ, large wavelengths: □, first-order Engquist and Majda NRBC; ———, present first-order nonlinear NRBC adapted to $\theta = 45°$ ($w^{(-)} = 1.41$, $w^{(+)} = 0.59$).

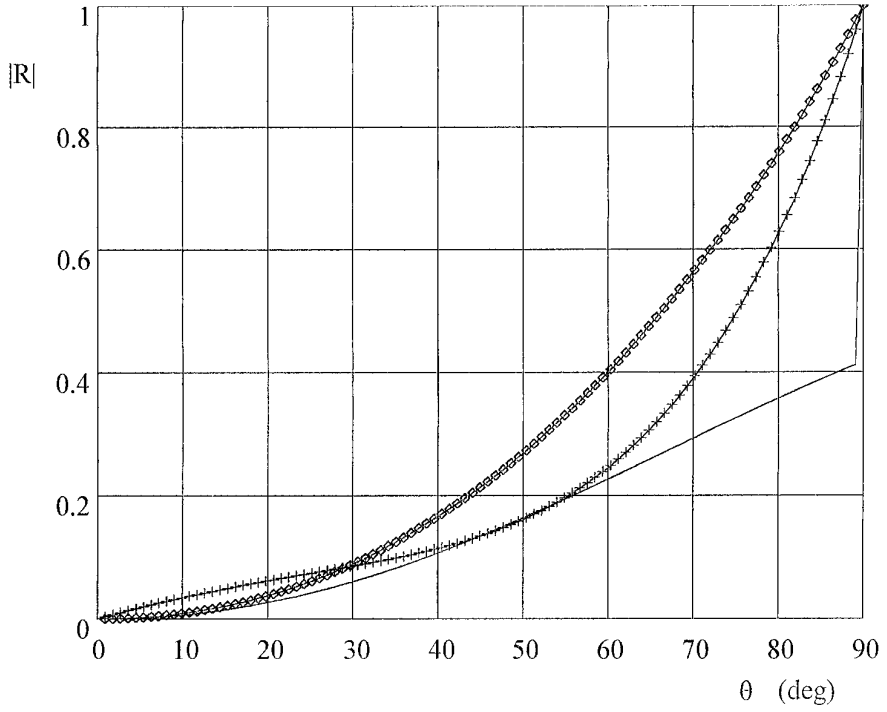

FIG. 2. First-order NRBCs, $|R|$ versus θ, $|\mathbf{k}| = \pi/(2h)$: □, first-order Engquist and Majda NRBC; −+−, present first-order nonlinear NRBC adapted to $\theta = 45°$ ($w^{(-)} = 1.41$, $w^{(+)} = 0.59$); ———, present first-order nonlinear NRBC with variable weights.

45°, but the obtained reflection is considerably lower than the reference value. Presented in this figure is also the curve relative to weights variable with θ and chosen according to Eq. (2.14).

2.2. *Second-Order Method*

The second-order analytical boundary condition of Engquist and Majda is obtained by selecting in Eq. (2.5), $m = 2$. As can be verified by using Taylor's series expansions, a first-order accurate discretization of this condition is given by

$$u_{0,j}^{(n+1)} = u_{1/2,j-1/2}^{(n)} + u_{1/2,j+1/2}^{(n)} - \tfrac{1}{4}(u_{1,j-1}^{(n-1)} + 2u_{1,j}^{(n-1)} + u_{1,j+1}^{(n-1)}). \tag{2.19}$$

As will be shown during the presentation of the results, it is interesting to note that this formula is different from the numerical discretization proposed by Engquist and Majda in [3] and Higdon in [4], although it is an approximation of the same differential equation.

The reflection coefficient of this boundary condition is

$$R = -\frac{[z^2 - zk_2^{1/2}(l^{-1/2} + l^{1/2}) + \tfrac{1}{4}k_2(l^{-1} + 2 + l)]}{[z^2 - zk_1^{1/2}(l^{-1/2} + l^{1/2}) + \tfrac{1}{4}k_1(l^{-1} + 2 + l)]} \tag{2.20}$$

and for large wavelengths it becomes

$$R \approx -\frac{(\omega + \alpha_2)^2}{(\omega + \alpha_1)^2} = -\frac{(1 - \cos\theta)^2}{(1 + \cos\theta)^2}. \tag{2.21}$$

The procedure adopted to develop the first-order nonlinear NRBC can be extended and applied to Eq. (2.19), giving the second-order nonlinear adaptive boundary condition:

$$\begin{aligned} u_{0,j}^{(n+1)} = {} & \tfrac{1}{2}(u_{1/2,j-1/2}^{(n)} + u_{1/2,j+1/2}^{(n)}) \\ & + \tfrac{1}{2}(w^{(-)}u_{1/2,j-1/2}^{(n)} + w^{(+)}u_{1/2,j+1/2}^{(n)}) \\ & - \tfrac{1}{4}[w^{(-)}(u_{1,j-1}^{(n-1)} + u_{1,j}^{(n-1)}) \\ & + w^{(+)}(u_{1,j}^{(n-1)} + u_{1,j+1}^{(n-1)})]. \end{aligned} \tag{2.22}$$

In this case the weights are computed by inserting the Taylor series expansion (2.11) into Eq. (2.22) with the second-order term included. Equating the coefficients of f_0, f_0', and f_0'' to zero we get the same expressions (2.14) of the weights that were obtained at first-order (the equation for f_0 is identically satisfied). The differential expression equivalent to Eq. (2.22) is

$$\begin{aligned} & [u_{xx} + u_{tt} - 2u_{xt} + \tfrac{1}{2}w^{(+)}(\tfrac{3}{2}u_{xy} + u_{yt}) \\ & \quad - \tfrac{1}{2}w^{(-)}(\tfrac{3}{2}u_{xy} + u_{yt})]_{x=0} = 0 \end{aligned} \tag{2.23}$$

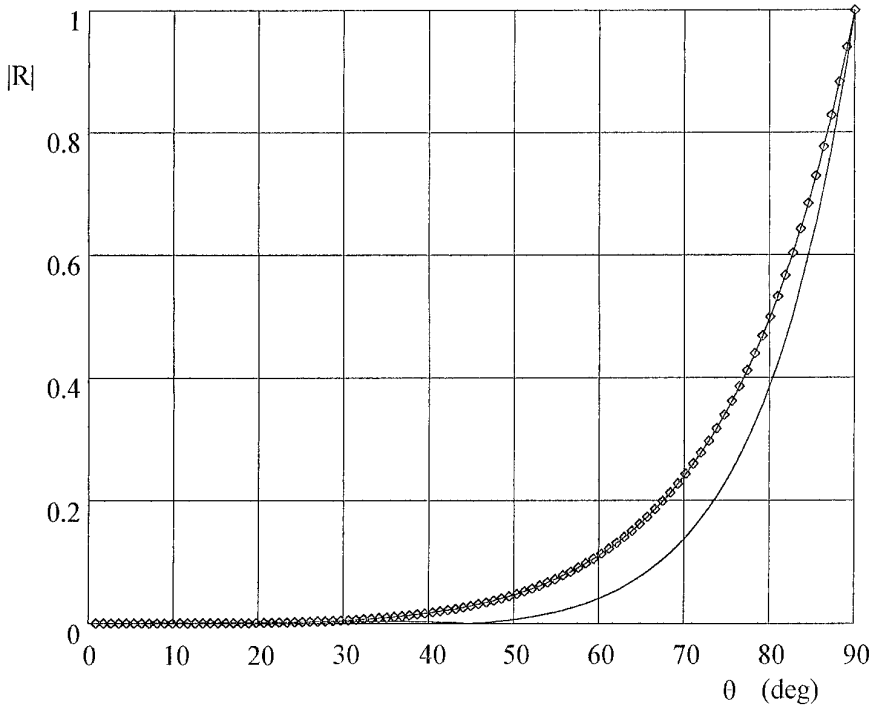

FIG. 3. Second-order NRBCs, $|R|$ versus θ, large wavelengths: □, second-order Engquist and Majda NRBC; ———, present second-order nonlinear NRBC adapted to $\theta = 45°$ ($w^{(-)} = 1.41$, $w^{(+)} = 0.59$).

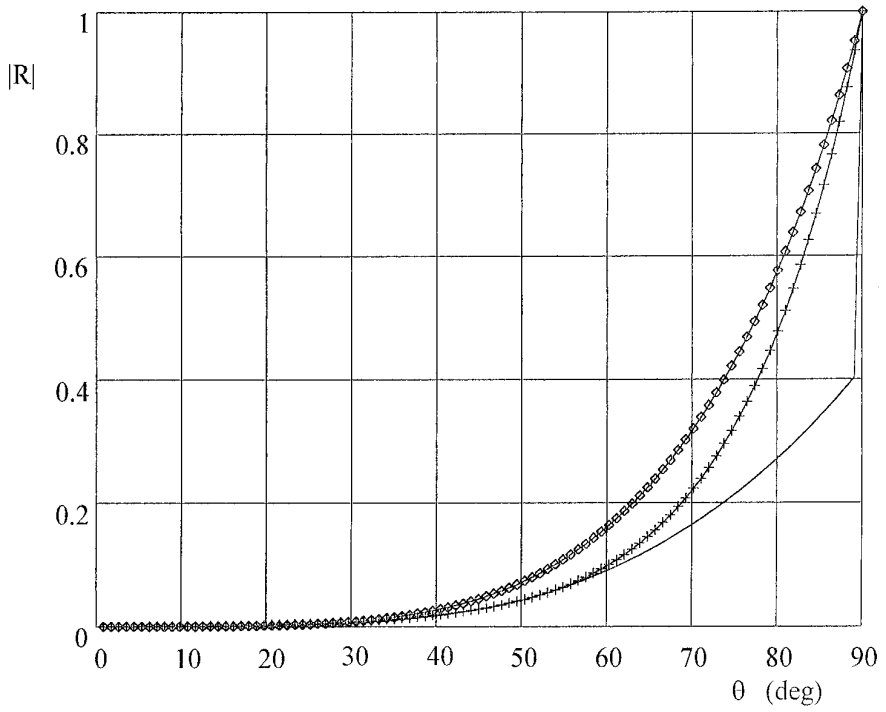

FIG. 4. Second-order NRBCs, $|R|$ versus θ, $|\mathbf{k}| = \pi/(2h)$: □, second-order Engquist and Majda NRBC; −+−, present second-order nonlinear NRBC adapted to $\theta = 45°$ ($w^{(-)} = 1.41$, $w^{(+)} = 0.59$); ———, present second-order nonlinear NRBC with variable weights.

and, for $w^{(-)} = w^{(+)}$ returns the original formula of Engquist and Majda.

The reflection coefficient of (2.22) is given by

$$R = -\frac{\begin{array}{c}\{z^2 - \frac{1}{2}zk_2^{1/2}[l^{-1/2}(1 + w^{(-)}) + l^{1/2}(1 + w^{(+)})] \\ + \frac{1}{4}k_2[w^{(-)}(l^{-1} + 1) + w^{(+)}(1 + l))]\}\end{array}}{\begin{array}{c}\{z^2 - \frac{1}{2}zk_1^{1/2}[l^{-1/2}(1 + w^{(-)}) + l^{1/2}(1 + w^{(+)})] \\ + \frac{1}{4}k_1[w^{(-)}(l^{-1} + 1) + w^{(+)}(1 + l))]\}\end{array}}. \tag{2.24}$$

For large wavelengths it becomes

$$\begin{aligned} R &\approx -\frac{\begin{array}{c}[(\omega + \alpha_2)^2 + \frac{1}{2}(w^{(+)} - w^{(-)})\alpha_2\beta \\ + \frac{1}{2}(w^{(+)} - w^{(-)})\omega\beta]\end{array}}{\begin{array}{c}[(\omega + \alpha_1)^2 + \frac{1}{2}(w^{(+)} - w^{(-)})\alpha_1\beta \\ + \frac{1}{2}(w^{(+)} - w^{(-)})\omega\beta]\end{array}} \\ &= -\frac{\begin{array}{c}[(1 - \cos\theta)^2 - \frac{1}{2}(w^{(+)} - w^{(-)})\sin\theta\cos\theta \\ + \frac{1}{2}(w^{(+)} - w^{(-)})\sin\theta]\end{array}}{\begin{array}{c}[(1 + \cos\theta)^2 + \frac{1}{2}(w^{(+)} - w^{(-)})\sin\theta\cos\theta \\ + \frac{1}{2}(w^{(+)} - w^{(-)})\sin\theta]\end{array}}. \end{aligned} \tag{2.25}$$

Diagrams corresponding to those provided for the second-order case are presented in Fig. 3 and Fig. 4, representing, respectively, the reflection coefficient behaviour given by Eq. (2.24) and Eq. (2.25). The general behaviour is similar to what was observed in the previous case. It is, however, evident, by comparing Figs. 1, 2 with Figs. 3, 4 that the second-order boundary conditions have even better absorbing properties.

3. NUMERICAL TEST RESULTS

The boundary conditions discussed in the previous section have been evaluated by numerical experiments performed on some of the same tests proposed by Higdon in [4].

Higdon's Test 1 has been slightly modified by increasing the distance of the far field from the source, thus obtaining a numerical experiment that better resembles the practical cases of the application of NRBCs.

The spatial domain was defined as

$$\Omega = \{(x, y): -0.96 < x < 4, -4 < y < 4\}$$

and discretized by a grid with constant mesh size $h = 0.08$. The boundary conditions were tested at the wall $x = -0.96$, whereas the reference solution without wall reflection effects was obtained in the domain $-4 < x < 4$, $-4 < y < 4$. During the time interval of the numerical test the left

TABLE I

Reflection Error as a Function of Time for Test 1

t	(a)	(b)	(c)	(d)
0.4	0	0	0	0
0.8	0.14	0.27	0	0.01
1.2	2.11	2.12	0.25	0.25
1.6	4.4	2.94	0.89	0.61
2	6.34	3.58	1.7	0.92
2.4	7.9	4.15	2.54	1.45
2.8	9.16	4.55	3.33	2.35
3.2	10.18	4.99	4.06	2.9

Note. (a)–(d) values are percentages.

boundary reflection only affected the data, since no perturbations reached to the other boundaries. The initial conditions assigned to the test problem are:

$$\begin{aligned} u(x_i, y_j, 0) &= e^{-30r_{i,j}^2} \quad \text{if } r_{i,j} < 0.45, \\ u(x_i, y_j, 0) &= 0 \quad \text{if } r_{i,j} \geq 0.45, \\ u_t(x_i, y_j, 0) &= 0, \end{aligned} \tag{3.1}$$

where $r_{i,j}^2 = x_i^2 + y_j^2$, $i = \{0, 1, 2, ..., 62\}$, $j = \{0, 1, 2, ..., 100\}$. The inner field difference scheme applied to solve the wave equation is the one previously described (Eq. (2.2)). The following boundary conditions were tested in turn:

(a) first-order BC, Eq. (2.6);
(b) first-order nonlinear adaptive BC, Eq. (2.10);
(c) second-order Engquist and Majda BC, Eq. (2.18);
(d) second-order nonlinear adaptive BC, Eq. (2.21).

The present results have been obtained without any special treatment of corner points, implying that at such points the boundary condition falls back on a first-order NRBC. A special treatment of corners consistent with the general method adopted for smooth boundaries can be devised if necessary.

In Table I the reflection errors obtained by the different methods at various times are presented. The reflection error is measured (as in [4]) by the L_2-norm of the difference between the test solution and reference solution vectors. In the table this error is expressed in percentage of the L_2-norm of the initial solution.

The results are in substantial agreement with the reflection level predicted by the theory. The reflection error of the first-order method (a) is significantly higher than the others; it is, however, strongly reduced by the nonlinear procedure (b), reaching a level slightly higher than the second-order linear method (c). The reflection is further reduced by using the second-order adaptive procedure (d). The improvement in accuracy obtainable by the present nonlinear procedures is also qualitatively shown by Figs. 5, 6, in which the isocurve plots of the solution at times $t = 1.6$ and $t = 3.2$ are presented for all the discussed NRBCs. Due to the polar symmetry of the analytical solution with respect to the source, the isocurve plots easily reveal the disturbances reflected by the left boundary, that, as is obvious, become more and more evident with increasing time. The high-frequency oscillations visible in the plots are an effect of the linear interpolation that the contouring algorithm uses to fit the discretized solution. We preferred to use such a simple algorithm and to have to filter out some noise visually rather than to obtain a possibly misleading, artificial smoothing from higher order interpolation.

The second test we have chosen corresponds to Test 3 proposed by Higdon. The domain is defined as

$$\Omega = \{(x, y): 0 < x < 2, -2 < y < 2\},$$

whereas the constant mesh size of the grid is now $h = 0.04$. The reference solution has been computed for $-1 < x < 2$, $-2 < y < 2$. In this case the L_2-norm of the reflection error is computed in a restricted region ($0 < x < 1$, $-1.5 < y < 1.5$) so that the reflections from the top, bottom, and right boundaries (and also from the left boundary for the reference solution) cannot influence the result for the time interval of the numerical test. The initial conditions of the difference problem are

$$\begin{aligned} u(x_i, y_j, 0) &= \cos(0.8i - 0.8j) \cdot e^{-30r_{i,j}^2} \quad \text{if } r_{i,j} < 0.45, \\ u(x_i, y_j, 0) &= 0 \quad \text{if } r_{i,j} \geq 0.45, \\ u_t(x_i, y_j, 0) &= 0, \end{aligned} \tag{3.2}$$

where $r_{i,j}^2 = (x_i - 0.5)^2 + (y_i + 0.5)^2$, $i = \{0, 1, 2, ..., 50\}$, $j = \{0, 1, 2, ..., 100\}$. This test involves a wave packet travelling at approximately 45° incidence, built out of high-frequency components.

As previously described, the correct computation of the wave direction for method (d) was obtained by smoothing the local gradient. In Table II the reflection errors for Test

TABLE II

Reflection Error as a Function of Time for Test 2

t	(a)	(b)	(c)	(d)	(e)
0.2	0.06	0.05	0.01	0.01	0.01
0.4	0.86	0.54	0.14	0.1	0.06
0.6	3.56	2.05	0.68	0.26	0.25
0.8	6.97	4.2	1.6	0.65	0.47
1	9.29	7.06	2.45	1.15	0.95
1.2	10.5	9.16	3.04	1.53	1.37
1.4	11.11	9.04	3.41	1.94	1.68
1.6	11.42	9.42	3.65	2.13	1.89

Note. (a)–(e) values are percentages.

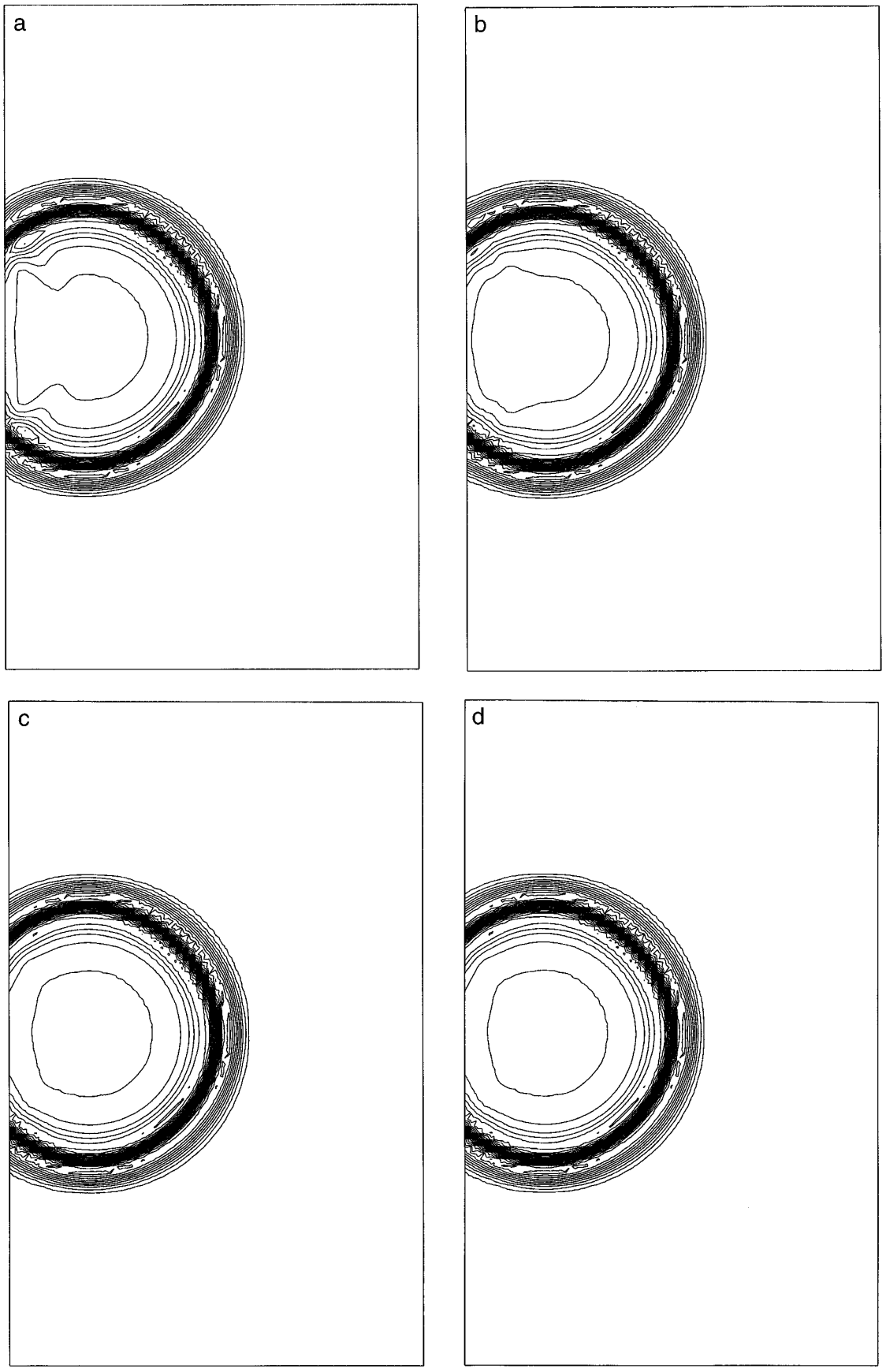

FIG. 5. Test 1, isocurves of the numerical solution at time $t = 1.6$ ($u_{\min} = -0.07$, $u_{\max} = 0.11$, $\Delta = 0.01$): (a) first-order Engquist and Majda NRBC; (b) present first-order nonlinear adaptive NRBC; (c) second-order Engquist and Majda NRBC; (d) present second-order nonlinear adaptive NRBC.

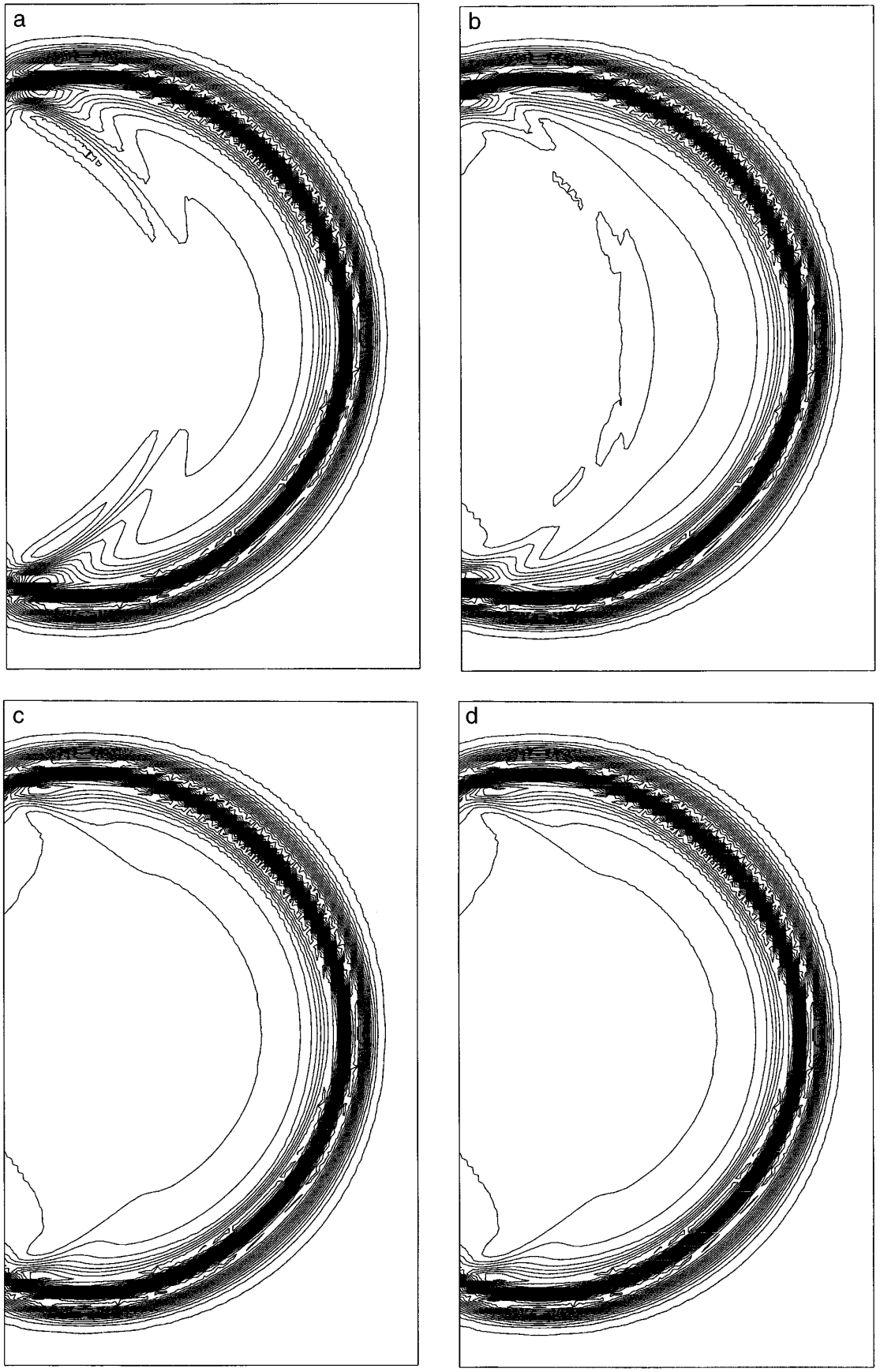

FIG. 6. Test 1, isocurves of the numerical solution at time $t = 3.2$ ($u_{\min} = -0.064$, $u_{\max} = 0.094$, $\Delta = 0.01$): (a) first-order Engquist and Majda NRBC; (b) present first-order nonlinear adaptive NRBC; (c) second-order Engquist and Majda NRBC; (d) present second-order nonlinear adaptive NRBC.

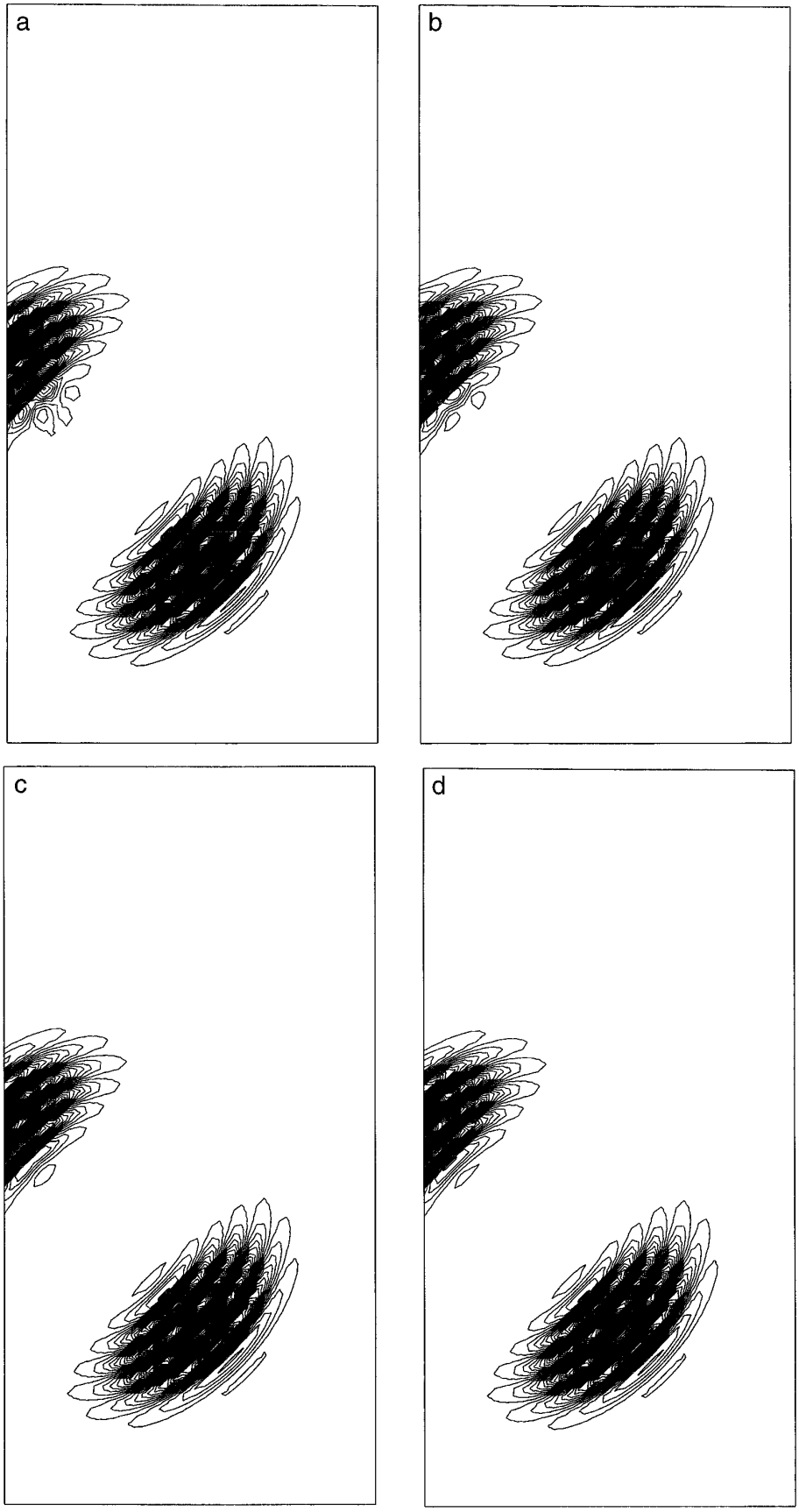

FIG. 7. Test 2, isocurves of the numerical solution at time $t = 0.8$ ($u_{\min} = -0.335$, $u_{\max} = 0.325$, $\Delta = 0.01$): (a) first-order Engquist and Majda NRBC; (b) present first-order nonlinear adaptive NRBC; (c) second-order Engquist and Majda NRBC; (d) present second-order nonlinear adaptive NRBC.

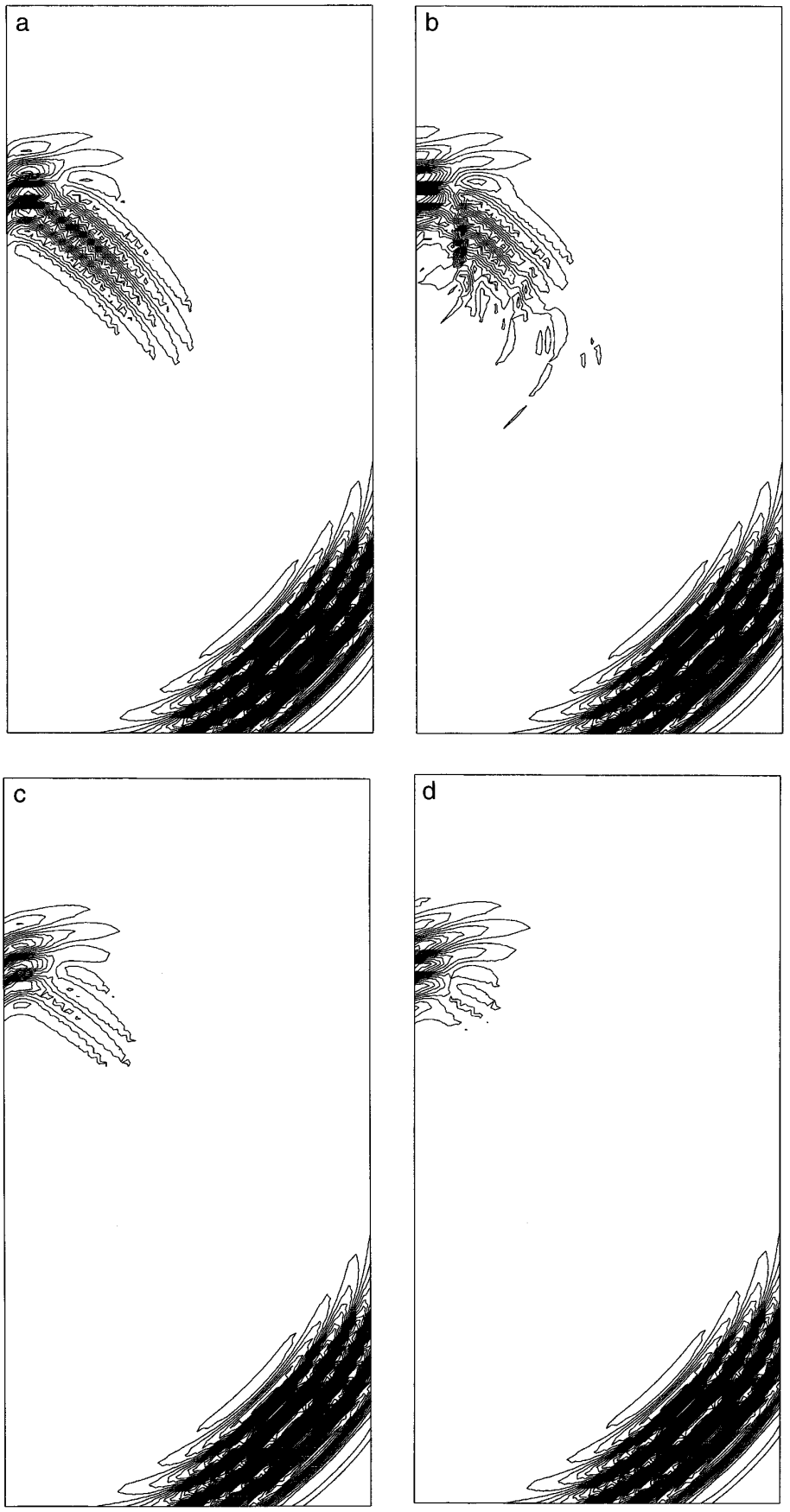

FIG. 8. Test 2, isocurves of the numerical solution at time $t = 1.6$ ($u_{\min} = -0.235$ $u_{\max} = 0.215$, $\Delta = 0.01$): (a) first-order Engquist and Majda NRBC; (b) present first-order nonlinear adaptive NRBC; (c) second-order Engquist and Majda NRBC; (d) present second-order nonlinear adaptive NRBC.

2 are reported. In this case another column has been added containing the results of method (e), consisting of formula (2.21) with constant weight values set to $w^{(-)} = 1.41$, $w^{(+)} = 0.59$, corresponding to 45° travelling waves. These results agree with the conclusions of the previous test: the best absorbing properties were provided by the second-order nonlinear adaptive method (d), as can be confirmed by isocurve plotting of the solutions obtained at time $t = 0.8$ and $t = 1.6$ and presented in Figs. 7, 8. The results obtained by the adaptive procedure (d) are very near the reflection errors presented in column (e), determined by an "a priori" knowledge of the direction of outgoing waves, thus confirming the correct design of the local wave direction computation.

Incidentally, it is interesting to compare the results of method (c) (the second-order Engquist and Majda's formula) with those presented by Higdon in [4, Table 6.3, columns (c) and (d)], relative to two different discretizations of the second-order Engquist and Majda NRBC: the classical one proposed in [3] and the difference approximation of Eq. (1.1) with $\theta_j = 0$. Although the results cannot be precisely compared, because different inner schemes and a different time step have been used, the Engquist and Majda NRBC, as implemented by Higdon, exhibits significantly worse reflection errors than our method (c). This discrepancy can only be due to the different discretization of the same analytical condition. It may be that the pyramidal six-point structure of our difference boundary operator better adapts to the domain of influence of the local outgoing wave.

4. CONCLUSIONS

The nonlinear adaptive NRBCs (first- and second-order) developed in this work appear to reduce the wave reflection error of classical NRBCs. In fact, despite the simplicity of the method, the reflection coefficients can be considerably reduced by choosing, as the total absorption direction at each time step, the locally estimated direction of the wave hitting the boundary.

Our expectations have been confirmed by the numerical experiments, in which the present nonlinear first- and second-order NRBCs have been compared with the first- and second-order Engquist and Majda methods that are typical examples of linear NRBCs, based on a local approach. The reflection errors have been significantly reduced by the nonlinear algorithms, whereas the computational cost was increased hardly at all by the gradient computation at the boundary.

REFERENCES

1. D. Givoli, *J. Comput Phys.* **94,** 1 (1991).
2. D. Givoli and D. Cohen, *J. Comput Phys.* **117,** 1 (1995).
3. B. Engquist and A. Majda, *Math. Comput.* **31,** 629 (1977).
4. R. L. Higdon, *Math. Comput.* **47,** 437 (1986).
5. R. L. Higdon, *J. Comput. Phys.* **101,** 2 (1992).